

Response of macroscopic and microscopic dynamical quantifiers to the quantum critical region

Stav Haldar¹, Saptarshi Roy¹, Titas Chanda^{1,2}, Aditi Sen(De)¹

¹Harish-Chandra Research Institute, HBNI, Chhatnag Road, Jhansi, Allahabad 211 019, India

²Instytut Fizyki im. Mariana Smoluchowskiego, Uniwersytet Jagielloński, Łojasiewicza 11, 30-348 Kraków, Poland.

At finite temperatures, the quantum critical region (QCR) emerges as a consequence of the interplay between thermal and quantum fluctuations. We seek for suitable physical quantities, which during dynamics can give prominent response to QCR in the transverse field quantum XY model. We report that the maximum energy absorbed, the nearest neighbor entanglement and the quantum mutual information of the time evolved state after a quench of the transverse magnetic field exhibits a faster fall off with temperature when the initial magnetic field is taken from within the QCR, compared to the choice of the initial point from different phases. We propose a class of dynamical quantifiers, originated from the patterns of these physical quantities and show that they can faithfully mimic the equilibrium physics, namely detection of the QCR at finite temperatures.

Introduction.- The onset of a phase transition is signalled by the emergence of long-range fluctuations in the system. In the classical domain, these fluctuations are solely driven by temperature leading to a phase transition when the temperature crosses a critical value. On the other hand, in the absolute zero temperature, where thermal fluctuations are completely absent, quantum phase transitions (QPTs) [1–3] can occur, which are exclusively driven by quantum fluctuations. Such transition typically takes place at specific value(s) of system parameter(s) called the quantum critical point(s) (QCP). The QCP in a QPT takes the analogous role of the critical temperature in case of classical phase transitions. It was recently found that the presence of QCP can interestingly induce nonanalyticities in the dynamics of physical quantities after a quench of system parameters in paradigmatic one-dimensional quantum spin models. The study of these dynamical nonanalyticities goes by the name of dynamical quantum phase transition (DQPT) [4–13], which was shown to be detected by Loschmidt echo [11] and entanglement measures [14, 15].

Typically, studies of phase transition hovers around two extremes: the high temperature (classical) limit and the zero temperature quantum limit. However, the story becomes interesting when one probes in regimes where both thermal and quantum fluctuations are finite. A complete understanding of the phases of the system where both of these fluctuations co-exist is an essential challenge that is yet to be resolved. Nevertheless, there has been a number of efforts to uncover the region, known as quantum critical region (QCR) [1], where both thermal and quantum effects are present. In the finite temperature domain, studying the canonical equilibrium state reveals that the quantum critical point expands into a conical region, the QCR, with the zero temperature QCP at its vertex. To detect such a region, no order parameter based classification or gap closing criterion exists, thereby making its identification extremely challenging. However, a few studies in this direction include detection through directional derivatives of magnetization and entanglement [16], via Benford analysis of magnetization [17], and a recent experimental observation of QCR [18]. Note that the properties of the QCR are dictated by scale invariance which it borrows from the underlying QCP. The boundaries of the QCR for low temperatures is defined

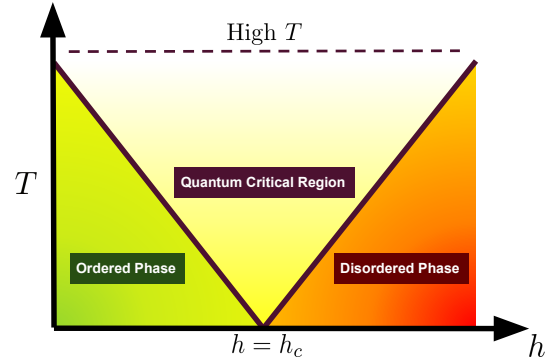


FIG. 1. (Color online.) A schematic representation of the quantum critical region (QCR), the ordered and disordered phases with respect to the system parameter h and temperature T . At zero temperature, the system undergoes a quantum phase transition from ordered to disordered phase at $h = h_c$. At high temperatures, strong thermal fluctuations typically washes out the quantum phases.

by the straight lines

$$T = C|h - h_c|, \quad (1)$$

where C is a constant determined by the universality class of the system [1], and h represents the system parameter, while $h = h_c$ denotes the QCP.

In this paper, we search for physical characteristics at finite temperatures which yield a well defined response to the QCR during their dynamics. We report that energy absorbed during a time pulse, a quantity of macroscopic origin, and microscopic information theoretic quantities like bipartite entanglement and quantum mutual information, manifest a qualitative difference in their dynamics when the initial quench point is “within” the QCR. Interestingly, the dynamical response of these quantities can be structured in a way which enables quantitative demarcation of the QCR.

Model.- We consider an interacting quantum spin-1/2 system on a one-dimensional (1D) lattice with nearest-neighbor anisotropic XY interaction in presence of a uniform external transverse magnetic field. The model is described by the

Hamiltonian

$$\hat{H} = \frac{1}{2} \sum_{j=1}^N \left[J \left(\frac{1+\gamma}{2} \hat{\sigma}_j^x \hat{\sigma}_{j+1}^x + \frac{1-\gamma}{2} \hat{\sigma}_j^y \hat{\sigma}_{j+1}^y \right) + h \hat{\sigma}_j^z \right] \quad (2)$$

with periodic boundary condition. Here, $\hat{\sigma}^\alpha$ with $\alpha = x, y, z$ are the Pauli matrices, J represents the strength of nearest-neighbor exchange interaction, γ ($\neq 0$) is the anisotropy parameter in the $x - y$ direction, h is the uniform transverse magnetic field strength, and N denotes the total number of lattice sites. The above Hamiltonian can be mapped to a spinless 1D Fermi system via the Jordan-Wigner transformation, and then can be solved exactly via successive Fourier and Bogoliubov transformations [19], for details, see Appendix A. For non zero choices of γ , the 1D quantum XY model at zero temperature has a QCP at $h/J = 1$ where the model undergoes from an ordered phase, a ferromagnetic one for $J < 0$ or an antiferromagnetic one for $J > 0$ (with $h < |J|$) to a disordered paramagnetic phase (when $h > |J|$). Here, we set out to investigate how the dynamics gets effected in a finite temperature situation due to the presence of QCR via both macroscopic and microscopic quantities.

Macroscopic signatures of QCR: Energy absorbed during a time pulse.- In the context of zero temperature QPT, it was shown [20] that the energy absorbed in a square pulse quench of the magnetic field (see below), in the long time limit develops some kinks when the quench crosses an equilibrium quantum critical point of the transverse field XY model. Therefore, this intrinsic non-equilibrium quantity could mimic equilibrium properties. This motivated us to investigate the features of this quantity at finite temperatures, and search for signatures of the QCR. We study dynamics of the canonical equilibrium state of temperature T , under a time pulse of the external transverse magnetic field of the form,

$$h(t) = \begin{cases} h_0, & t \leq 0, \\ h_1, & 0 < t \leq \tau, \\ h_0, & t > \tau, \end{cases} \quad (3)$$

i.e., the initial Hamiltonian \hat{H}_0 corresponding to a transverse field strength h_0 is quenched to a new hamiltonian \hat{H}_1 with transverse field strength h_1 . The time evolution of the thermal state of \hat{H}_0 at a temperature T is allowed to take place with \hat{H}_1 for a finite time τ . Finally, the external field is quenched back to its original value h_0 . Since the XY model is integrable, the time evolved state at time τ can be calculated analytically, and allows one to evaluate the energy absorbed during the time pulse, which is defined as

$$\Delta E(T, \tau) = \text{Tr}(\hat{H}_0 e^{-i\hat{H}_1 \tau} \hat{\rho}_0 e^{i\hat{H}_1 \tau}) - \text{Tr}(\hat{H}_0 \hat{\rho}_0), \quad (4)$$

where $\hat{\rho}_0 = e^{-\frac{\hat{H}_0}{k_B T}} / \text{Tr} e^{-\frac{\hat{H}_0}{k_B T}}$, with k_B being the Boltzmann constant, represents the thermal state. After performing Jordan-Wigner and Fourier transformations, the Hamiltonian reduces to different momentum blocks consisting of 4×4 matrices, i.e., $\hat{H} = \sum_p \hat{H}_p$ (see Appendix A), and hence Eq. (4)

in terms of the momentum blocks reads as

$$\Delta E(T, \tau) = \frac{1}{2\pi} \int dp [\text{Tr}(\hat{H}_0^p e^{-i\hat{H}_1^p \tau} \rho_0^p e^{i\hat{H}_1^p \tau}) - \text{Tr}(\hat{H}_0^p \rho_0^p)]. \quad (5)$$

The value of the absorbed energy maximized over the duration of the pulse can be calculated as

$$\Delta E_{\max}(T) = \max_{\tau} |\Delta E(T, \tau)|. \quad (6)$$

In order to reveal the equilibrium QCR, we analyze the temperature dependence of the scaled quantity

$$\Delta \tilde{E}(T) = \frac{\Delta E_{\max}(T)}{\Delta E_{\max}(T=0)}. \quad (7)$$

The above quantity depends both on the initial and final fields (h_0 and h_1) and consequently on their corresponding phases. To obtain proper response for equilibrium QCR, the final quench point should be chosen suitably such that it maximizes the distinct temperature dependence of $\Delta \tilde{E}(T)$. We find that choosing the final quench point as $h_1/J = 1$ gives rise to strong temperature dependence of $\Delta \tilde{E}(T)$ for almost any choice of the initial quench point h_0 , and hence we fix $h_1/J = 1$ for all our quantitative analyses. However, the qualitative features reported here remains unaltered even for different values of the final field strength h_1 as we will see later. Therefore, we are left with a quantity that effectively depends on only the (h_0, T) -pair. We would use this pair to demarcate the QCR later in this paper. Nevertheless, the qualitative findings (see Fig. 2 (a)) of our investigation using $\Delta \tilde{E}(T)$, for $k_B T/J \lesssim 0.1$, is summarized below:

1. If the initial field strength, h_0 , is chosen from deep inside the ordered or disordered phases, $\Delta \tilde{E}(T)$ is an almost constant function of T , i.e., it changes negligibly with changing temperature.
2. If h_0 is inside the quantum critical region, i.e. from points close to the quantum critical point, there is a rapid fall of $\Delta \tilde{E}(T)$ with temperature. The closer the initial quench point is to the QCP, the faster the fall.
3. The relevant physics reported in 1 and 2 above is independent of the quench length, $|h_0/J - h_1/J|$, in the sense that they do not effect the fall off feature in $\Delta \tilde{E}(T)$. For example, for the quench: $h_0/J(0.2) \rightarrow h_1/J(0.3, 2)$, we get that all the relevant quantities under consideration remain almost constant for $\frac{k_B T}{J} \lesssim 0.1$, while for the quench: $h_0/J(0.95) \rightarrow h_1/J(0.3, 2)$, we observe a rapid fall off in $\Delta \tilde{E}$. See Fig. 3. As mentioned earlier, the choice of $h_1 = J$ was motivated by the observation that driving by the Hamiltonian with critical parameters yield a strong response to the QCR. Similar behavior can also be seen with microscopic quantities, which are discussed later in the manuscript.

On the other hand, for higher temperatures, the thermal fluctuations surpass its quantum counterparts and the signatures

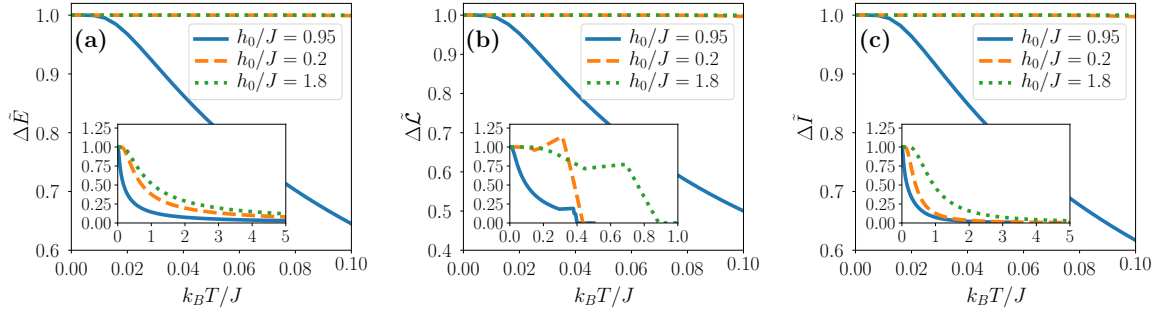


FIG. 2. (Color online.) Temperature dependence of $\Delta\tilde{Q} = \frac{\Delta Q_{\max}(T)}{\Delta Q_{\max}(T=0)}$ for a given physical quantity, Q . The abscissa represent $k_B T/J$ and the ordinate is $\Delta\tilde{Q}$. (a) Q is the energy absorbed during a time pulse, (b) $Q =$ logarithmic negativity, (c) $Q =$ quantum mutual information. Plots are for different values of h_0/J and a fixed value of the final quench parameter $h_1/J = 1$. For $k_B T/J \lesssim 0.1$, $\Delta\tilde{Q}$ falls sharply when the quench begins from the QCR whereas it is almost independent of temperature when the quench begins from the ordered and disordered regimes. For higher temperatures, $\Delta\tilde{E}$ and $\Delta\tilde{I}$ reach zero asymptotically, as depicted in inset (a) and (c), while $\Delta\tilde{L}$ displays nonmonotonicity and sudden collapse with respect to T , shown in inset (b). All axes are dimensionless.

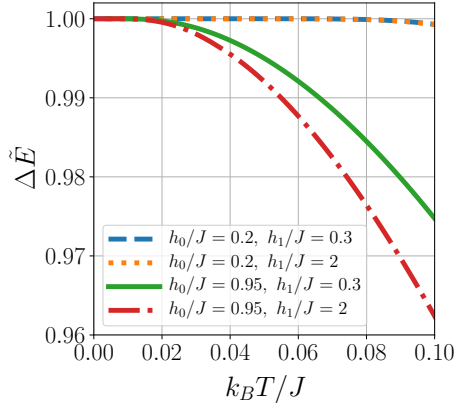


FIG. 3. (Color online.) Independence of the fall off feature in $\Delta\tilde{E}$. The abscissa represents temperature, $k_B T/J \lesssim 0.1$, while the ordinate represents $\Delta\tilde{E}$. $\Delta\tilde{E}$ is calculated for different choices of $(h_0/J, h_1/J)$ -pair. The behavior of $\Delta\tilde{E}$ clearly shows that the characteristic temperature dependence is independent of the quench length $|h_0/J - h_1/J|$. Both axes are dimensionless.

of QCR vanish beyond a certain temperature. In particular, for any quenches beginning either in ordered, disordered or in QCR, the physical quantity of interest decreases almost identically with increasing temperature and vanishes asymptotically, see inset of Fig. 2 (a).

Microscopic signatures of QCR: entanglement and mutual information.— Let us now consider the dynamics of these microscopic quantities under the quenching strategy,

$$h(t) = \begin{cases} h_0, & t \leq 0 \\ h_1, & t > 0 \end{cases}. \quad (8)$$

Owing to the translational invariance of the model, all nearest neighbor density matrices of the initial as well as the time evolved states, $\hat{\rho}_{AB}(t, T)$, are identical (see Appendix A).

We start of our analysis with bipartite entanglement [21], which have been known to play an important role in detect-

ing equilibrium QCPs [22–28], although it turns out to be less effective in the case of dynamical phase transition at zero temperature [15]. Furthermore, in thermal equilibrium, entanglement has been used to detect the QCR [16]. Therefore, it is important to explore dynamical response of entanglement due to QCR. To quantify entanglement, we use negativity (\mathcal{N}) and logarithmic negativity (\mathcal{L}) [29–31], which are defined for an arbitrary two party density matrix ρ_{AB} , as

$$\begin{aligned} \mathcal{N}(\hat{\rho}_{AB}) &= \frac{1}{2}(\|\hat{\rho}_{AB}^{T_B}\| - 1) = \frac{1}{2}(\|\hat{\rho}_{AB}^{T_A}\| - 1), \\ \mathcal{L}(\hat{\rho}_{AB}) &= \log_2(2\mathcal{N}(\hat{\rho}_{AB}) + 1), \end{aligned} \quad (9)$$

where $\|A\| = \text{Tr}\sqrt{A^\dagger A}$ and $T_A(T_B)$ denotes partial transposition with respect to party $A(B)$ [32, 33]. The dynamics of nearest neighbor negativity as well as logarithmic negativity after a sudden quench as in Eq. (8), can be computed analytically in terms of classical correlators $C^{ij} = \text{Tr}(\hat{\rho}_{AB}(t, T)\sigma^i \otimes \sigma^j)$ with $i, j = x, y, z$, and the magnetization in the z direction, $m^z = \text{Tr}(\hat{\rho}_{AB}(t, T)\mathbb{I}_2 \otimes \sigma^z) = \text{Tr}(\hat{\rho}_{AB}(t, T)\sigma^z \otimes \mathbb{I}_2)$ (see Appendix A). The exact diagonalization of \hat{H} guarantees the analytical forms of the nonvanishing classical correlators and magnetization. Like in the case of energy absorbed, we consider the maximal value of logarithmic negativity which is defined as

$$\Delta\mathcal{L}_{\max}(T) = \max_t |\mathcal{L}(T, t) - \mathcal{L}(T, t=0)|, \quad (10)$$

and the corresponding scaled quantity as

$$\Delta\tilde{\mathcal{L}}(T) = \frac{\Delta\mathcal{L}_{\max}(T)}{\Delta\mathcal{L}_{\max}(T=0)}. \quad (11)$$

For low temperatures, $k_B T/J \lesssim 0.1$, $\Delta\tilde{\mathcal{L}}(T)$ also remain constant when the initial field strength is taken far from QCP while it decreases with $k_B T/J$ when h_0/J is chosen from the QCR (as depicted in Fig. 2 (b)). However, unlike $\Delta\tilde{E}(T)$, we notice that above $k_B T/J > 0.1$, $\Delta\tilde{\mathcal{L}}(T)$ reveals nonmonotonic behavior, see Fig. 2 (b), as reported in various earlier works in the static scenario [27, 28]. Furthermore, at

high temperatures, $\Delta\tilde{\mathcal{L}}(T)$ suddenly collapses to vanishingly small values which is not the case for $\Delta\tilde{E}(T)$, which in turn approaches zero asymptotically, comparing insets of Figs. 2 (a) and 2 (b).

We move on with our search for physical quantities and consider quantum mutual information [34] for the same. Unlike entanglement, which solely measures the quantum correlations, mutual information, $\mathcal{I}_{A:B}$, is a measure of the total correlations between A and B [35, 36]. For a bipartite density matrix $\hat{\rho}_{AB}$, the mutual information is defined as

$$\mathcal{I}_{A:B} = S(\hat{\rho}_A) + S(\hat{\rho}_B) - S(\hat{\rho}_{AB}) \quad (12)$$

where $S(\hat{\sigma}) = -\text{Tr}[\hat{\sigma} \log_2 \hat{\sigma}]$ is the von Neumann entropy of a state $\hat{\sigma}$, and $\hat{\rho}_{A(B)}$ is the reduced density matrices of $\hat{\rho}_{AB}$. Like in the previous cases, the mutual information of $\hat{\rho}_{AB}(t, T)$ can be evaluated in terms of its spectra analytically (see Appendix A). The maximum of the change in mutual information and its scaled variant for a given temperature T are defined respectively as

$$\begin{aligned} \Delta\mathcal{I}_{\max}(T) &= \max_t |\mathcal{I}_{A:B}(T, t) - \mathcal{I}_{A:B}(T, t=0)|, \\ \Delta\tilde{\mathcal{I}}(T) &= \frac{\Delta\mathcal{I}_{\max}(T)}{\Delta\mathcal{I}_{\max}(T=0)}, \end{aligned} \quad (13)$$

which again decreases with the variation of temperature when $h_0 \in \text{QCR}$, as depicted in Fig. 2 (c).

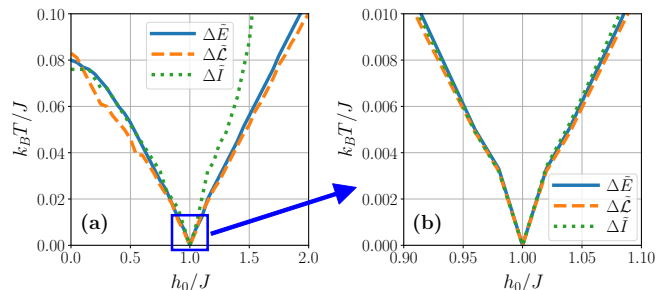


FIG. 4. (Color online.) Quantum critical region in the $(h_0/J, k_B T/J)$ -plane. It is constructed by solving Eq. (14) with energy absorbed, logarithmic negativity and quantum mutual information. For (a), temperature, $k_B T/J \lesssim 0.1$, while in (b), $k_B T/J$ is plotted upto 0.01. Both the axes are dimensionless.

Revealing the QCR using dynamical quantifiers. - We can now qualitatively discern amongst the different regimes of the equilibrium phase diagram viz. ordered, disordered and quantum critical regions by the distinct temperature dependence of the macroscopic and microscopic quantifiers, $\Delta\tilde{\mathcal{Q}}$, for different quantifiers \mathcal{Q} . With this qualitative success, it can be expected that it would also be possible to estimate the extent of the quantum critical regime quantitatively by studying the dynamics. The main observation that we obtain till now is that $\Delta\mathcal{Q}_{\max}(T) \approx \Delta\mathcal{Q}_{\max}(T=0)$ for $0 \leq T \leq T^*$, where T^* is fixed by the initial field strength, h_0 . We now propose that given a quantifier, \mathcal{Q} , and a value of h_0 , the boundary of the QCR can be indicated by the temperature T^* upto which the constancy window lasts. T^* can be computed from the

solution of the following condition:

$$\frac{|\Delta\mathcal{Q}_{\max}(T) - \Delta\mathcal{Q}_{\max}(T=0)|}{|\Delta\mathcal{Q}_{\max}(T=0)|} = \eta. \quad (14)$$

In principle, η should be zero, but numerically, it is chosen to be as close as possible to zero. Since evaluation of T^* from Eq. (14) is basically a root finding problem, η turns out to be the tolerance whose smallness is limited by numerical precision. In our analysis, we fix η to be 5×10^{-5} . Physically, it means that if the fractional change in $\Delta\mathcal{Q}(T)$ is below the cutoff η , it is considered to be constant, while $\eta > 5 \times 10^{-5}$ implies entry into the QCR. Let us now investigate whether such proposal works by studying the trends of $\mathcal{Q} \in \{E, \mathcal{L}, \mathcal{I}\}$.

Note that the QCR obtained from $\mathcal{Q} \in \{E, \mathcal{L}, \mathcal{I}\}$, i.e. from $\Delta\tilde{E}(T)$, $\Delta\tilde{\mathcal{L}}(T)$ and $\Delta\tilde{\mathcal{I}}(T)$ are qualitatively similar, i.e., the demarcated regions have a large overlap, see Figs. 4(a) and 4(b). Specifically, the QCR perfectly follows Eq. (1) in the range $k_B T/J \in [0, 0.01]$ with the slopes being $C_E = (0.121 \pm 0.004)$, $C_{\mathcal{L}} = (0.117 \pm 0.004)$, and $C_{\mathcal{I}} = (0.126 \pm 0.004)$ respectively for the three different quantifiers, where C_E , $C_{\mathcal{L}}$, and $C_{\mathcal{I}}$ are obtained from energy absorbed, entanglement and quantum mutual information respectively. We want to point out that these small quantitative differences are not at all alarming but rather expected, since the boundary of the QCR is not at all sharp, and there is an intrinsic fuzziness. The fact that there exists no order parameter or gap closing argument as in the case of zero temperature QPTs further reinforces the above statement. In reality, the uncanny similarities in the QCR as detected by quantities, which are chosen from different paradigms, one thermodynamic and the others microscopic, are rather remarkable.

Conclusion. - The coexistence of thermal and quantum fluctuations in the quantum critical region (QCR) makes the study of quantum phases in this regime very interesting. Although the proposal of QCR was made since the discovery of quantum phase transitions, due to the lack of any conclusive marker, very few investigations were made in this direction. Nonetheless, some attempts were made to study the QCR in equilibrium using varied techniques.

In this paper, we investigated the effect of QCR on the dynamics of physical quantities after a sudden quench of the system parameters. We reported a macroscopic quantity, namely the energy absorbed during a time pulse, and two microscopic ones from the information theoretic domain - entanglement (a measure of quantum correlations) and quantum mutual information (a measure of total correlations), which provide well defined and qualitatively similar response to the presence or absence of the QCR. We quantified their responses, and converted them into detection criterion for obtaining the boundary of QCR. These quantities, which lie completely on opposite ends of the spectrum distinguish the QCR from other phases efficiently.

We believe, our work can shed some light on the understanding of the coveted QCR. The proposal of dynamical quantifiers is relevant not only from the perspective of experimental feasibility, but also because they provide fundamental insights into the dynamical behavior of quantum critical matter.

ACKNOWLEDGMENTS

The authors thank Ujjwal Sen for useful discussions. TC was supported by Quantera QTFLAG project 2017/25/Z/ST2/03029 of National Science Centre (Poland).

Appendix A: Model Diagonalization: Computation of absorbed energy, mutual information, and entanglement

We consider a quantum XY model on a one dimensional (1D) lattice with N sites, described by a Hamiltonian,

$$\hat{H} = \frac{1}{2} \sum_{j=1}^N \left[J \left\{ \frac{1+\gamma}{2} \hat{\sigma}_j^x \hat{\sigma}_{j+1}^x + \frac{1-\gamma}{2} \hat{\sigma}_j^y \hat{\sigma}_{j+1}^y \right\} + h(t) \hat{\sigma}_j^z \right] \quad (\text{A1})$$

To diagonalize the XY model, it can be mapped to a free Fermi gas Hamiltonian by the Jordan-Wigner transformation in terms of the fermionic operator [19, 37–39], \hat{c} , as

$$\hat{H} = \frac{J}{2} \sum_{j=1}^N \left[\hat{c}_j^\dagger \hat{c}_{j+1} + \hat{c}_{j+1}^\dagger \hat{c}_j + \gamma (\hat{c}_j^\dagger \hat{c}_{j+1}^\dagger + \hat{c}_{j+1} \hat{c}_j) + \frac{h(t)}{J} (2\hat{c}_j^\dagger \hat{c}_j - 1) \right]. \quad (\text{A2})$$

Further a Fourier transformation enables us to write $\hat{H} = \sum_p \hat{H}_p$, where the matrix form of \hat{H}_p in the basis $\{|0\rangle, \hat{c}_p^\dagger \hat{c}_{-p}^\dagger |0\rangle, \hat{c}_p^\dagger |0\rangle, \hat{c}_{-p}^\dagger |0\rangle\}$, is given by

$$\hat{H}_p = J \begin{bmatrix} -h(t)/J & i\gamma \sin \phi_p & 0 & 0 \\ -i\gamma \sin \phi_p & h(t)/J + 2 \cos \phi_p & 0 & 0 \\ 0 & 0 & \cos \phi_p & 0 \\ 0 & 0 & 0 & \cos \phi_p \end{bmatrix}, \quad (\text{A3})$$

where $\phi_p = 2\pi p/N$.

Using this simplified form of the block diagonal Hamiltonian, we can easily compute the two-site nearest-neighbor reduced density matrix between j^{th} and $(j+1)^{\text{th}}$ lattice sites of the thermal state (at a temperature T) in equilibrium as

$$\hat{\rho}_{j,j+1}(T) = \frac{1}{4} \left[\mathbb{I}_j \otimes \mathbb{I}_{j+1} + m^z(T) (\hat{\sigma}_j^z \otimes \mathbb{I}_{j+1} + \mathbb{I}_j \otimes \hat{\sigma}_{j+1}^z) + \sum_{\alpha, \alpha' = x, y, z} C^{\alpha\alpha'}(T) \hat{\sigma}_j^\alpha \otimes \hat{\sigma}_{j+1}^{\alpha'} \right], \quad (\text{A4})$$

where $m^z(T) = \langle \hat{\sigma}_j^z \otimes \mathbb{I}_{j+1} \rangle_T = \langle \mathbb{I}_j \otimes \hat{\sigma}_{j+1}^z \rangle_T$ is the transverse magnetization (along the z -direction) and $C^{\alpha\alpha'}(T) = \langle \hat{\sigma}_j^\alpha \otimes \hat{\sigma}_{j+1}^{\alpha'} \rangle_T$ (with α and α' taking values x, y or z independently) are the classical correlators. Note that for any thermal state of the XY model, m^x, m^y and off diagonal classical correlators are identically zero. The translation invariance of the model assures all two site reduced density matrices to be identical, and consequently all the classical correlators and magnetizations to be site independent. Thus, we drop the site

labels and call the nearest neighbor density matrix to be ρ_{AB} . However, under sudden quenches,

$$h(t) = \begin{cases} h_0, & t \leq 0 \\ h_1, & t > 0 \end{cases}. \quad (\text{A5})$$

C^{xy} and C^{yx} also take finite values. The time evolved two site reduced density matrix, $\hat{\rho}_{AB}(t, T)$, can be computed by tracking the time evolution of the classical correlators and magnetization, which reads as

$$\begin{aligned} \hat{\rho}_{AB}(t, T) &= \frac{1}{4} \left[\mathbb{I}_A \otimes \mathbb{I}_B + m^z(t, T) (\hat{\sigma}_A^z \otimes \mathbb{I}_B + \mathbb{I}_A \otimes \hat{\sigma}_B^z) \right. \\ &+ \sum_{\alpha = x, y, z} C^{\alpha\alpha}(t, T) \hat{\sigma}_A^\alpha \otimes \hat{\sigma}_B^\alpha \\ &+ C^{xy}(t, T) \hat{\sigma}_A^x \otimes \hat{\sigma}_B^y + C^{yx}(t, T) \hat{\sigma}_A^y \otimes \hat{\sigma}_B^x \left. \right]. \end{aligned} \quad (\text{A6})$$

The time dependence of these quantities $m^z(t, T)$ and the classical correlators) after a sudden quench is analytically computed in [19, 38, 39]. Furthermore, for the XY model, we have $C^{xy}(t, T) = C^{yx}(t, T)$ for all times.

1. Evaluation of energy absorbed in a time pulse

The energy absorbed in a square time pulse that last a time τ is evaluated as

$$\Delta E(T, \tau) = \text{Tr}(\hat{H}_0 e^{-i\hat{H}_1 \tau} \rho_0 e^{i\hat{H}_1 \tau}) - \text{Tr}(\hat{H}_0 \rho_0) \quad (\text{A7})$$

where $\rho_0 = e^{-\frac{\hat{H}_0}{k_B T}} / \text{Tr} e^{-\frac{\hat{H}_0}{k_B T}}$. Now, after Fourier transformation, we have

$$\Delta E(T, \tau) = \frac{1}{2\pi} \int dp [\text{Tr}(\hat{H}_0^p e^{-i\hat{H}_1^p \tau} \rho_0^p e^{i\hat{H}_1^p \tau}) - \text{Tr}(\hat{H}_0^p \rho_0^p)], \quad (\text{A8})$$

where, $\hat{H}_{0,1}^p$ is obtained from Eq. (A3). This enormously simplifies the calculation since operators in each momentum block are just 4×4 matrices. The exponentials can be computed by diagonalizing the operators in the exponent by appropriate unitary operation, which leads to the following expression for $E(T, \tau)$:

$$E(T, \tau) = \frac{1}{2\pi} \int dp [\text{Tr}(\mathcal{U} \hat{H}_0^p \mathcal{U}^\dagger e^{-i\hat{H}_1^p \tau} \mathcal{U} \rho_0^p \mathcal{U}^\dagger e^{i\hat{H}_1^p \tau}) - \text{Tr}(\hat{H}_0^p \rho_0^p)], \quad (\text{A9})$$

where we have

$$\begin{aligned} \hat{H}_{0,1}^p &= \text{diag}(\cos \phi_p - \Lambda_{0,1}, \cos \phi_p + \Lambda_{0,1}, \cos \phi_p, \cos \phi_p), \\ e^{\pm i\hat{H}_1^p \tau} &= e^{\pm i\tau \cos \phi_p} \text{diag}(e^{\mp i\tau \Lambda_1}, e^{\pm i\tau \Lambda_1}, 1, 1), \\ \Lambda_{0,1} &= \sqrt{(\cos \phi_p + h_{0,1})^2 + \gamma^2 \sin^2 \phi_p}. \end{aligned} \quad (\text{A10})$$

Furthermore, the unitary $\mathcal{U} = U_1^\dagger U_0 \oplus \mathbb{I}_2$, where $U_{0,1}$ reads as

$$U_{0,1} = \frac{1}{\sqrt{2\Lambda_{0,1}}} \begin{bmatrix} i\sqrt{\Lambda_{0,1} + \alpha_{0,1}} & i\sqrt{\Lambda_{0,1} - \alpha_{0,1}} \\ -\sqrt{\Lambda_{0,1} - \alpha_{0,1}} & \sqrt{\Lambda_{0,1} + \alpha_{0,1}} \end{bmatrix}, \quad (\text{A11})$$

with $\alpha_{0,1} = h_{0,1} + \cos \phi_p$. Note that $U_{0,1} \oplus \mathbb{I}_2$ is the unitary which diagonalizes $\hat{H}_{0,1}^p$. Once we get $\hat{H}_0^p, \tilde{\rho}_0^p$ can be written as $e^{-\beta \hat{H}_0^p} / \text{Tr} e^{-\beta \hat{H}_0^p}$, and can be computed easily.

2. Evaluation of entanglement

For $\hat{\rho}_{AB}(t, T)$, we always get a state in which the only non-zero local magnetization is in the z -direction, $m^z(t, T)$. possess the following correlation matrix

$$\mathcal{T}(t, T) = \begin{bmatrix} C^{xx}(t, T) & C^{xy}(t, T) & 0 \\ C^{yx}(t, T) & C^{yy}(t, T) & 0 \\ 0 & 0 & C^{zz}(t, T) \end{bmatrix}, \quad (\text{A12})$$

$$\mathcal{N}(\hat{\rho}_{AB}(t, T)) = -\frac{1}{4} \min \left[0, 1 + C^{zz}(t, T) - \sqrt{(C^{xx}(t, T) + C^{yy}(t, T))^2 + 4(m^z(t, T))^2}, \right. \\ \left. 1 - C^{zz}(t, T) - \sqrt{(C^{xx}(t, T) - C^{yy}(t, T))^2 + 4(C^{xy}(t, T))^2} \right]. \quad (\text{A13})$$

Logarithmic negativity [31] is then easily calculated to be $\mathcal{L}(t, T) = \log_2(2\mathcal{N}(\hat{\rho}_{AB}(t, T)) + 1)$.

3. Evaluation of mutual information

For computing the mutual information, we first evaluate the spectrum of $\hat{\rho}_{AB}(t, T)$, and its single site reductions, $\hat{\rho}_A(t, T) = \text{Tr}_B \hat{\rho}_{AB}(t, T)$ which is equal to $\hat{\rho}_B(t, T) = \text{Tr}_A \hat{\rho}_{AB}(t, T)$. The spectrum of $\hat{\rho}_{AB}(t, T)$, $\mathcal{X}_{\hat{\rho}_{AB}(t, T)}$, is obtained from the eigenvalues of $\hat{\rho}_{AB}(t, T)$ and is given by

$$\mathcal{X}_{\hat{\rho}_{AB}(t, T)} = \frac{1}{4} \times \left\{ 1 - C^{zz}(t, T) \pm |C^{xx}(t, T) + C^{yy}(t, T)|, 1 + C^{zz}(t, T) \right. \\ \left. \pm \sqrt{(C^{xx}(t, T) - C^{yy}(t, T))^2 + 4(m^z(t, T))^2} \right\}. \quad (\text{A14})$$

with $C^{xy}(t, T) = C^{yx}(t, T)$. The computation of entanglement simplifies with the observation that $\hat{\rho}_{AB}(t, T)$ can be brought in the standard X -state [40, 41] form (diagonal correlation matrix with non-zero magnetization in the z -direction) by choosing appropriate unitaries in the local $x - y$ sectors. It is equivalent to the diagonalization of the upper 2×2 block of $\mathcal{T}(t, T)$. Since we have $m^x(t, T) = m^y(t, T) = 0$ to be identically 0, they would remain so for all bases in the $x - y$ plane. Furthermore, basis transformation in the local $x - y$ planes would keep $m^z(t, T)$ and $C^{zz}(t, T)$ unaltered. Since entanglement remains unchanged by local unitary operations, we compute the same for $\hat{\rho}_{AB}(t, T)$ using negativity [30], and it reads as

The spectra of $\hat{\rho}_{A(B)}(t, T)$ is computed to be

$$\mathcal{X}_{\hat{\rho}_A(t, T)} = \mathcal{X}_{\hat{\rho}_B(t, T)} = \frac{1}{2} \{1 \pm m^z(t, T)\}. \quad (\text{A15})$$

Therefore, the mutual information between A and B of $\hat{\rho}_{AB}(t)$ can be expressed as

$$\mathcal{I}_{A:B}(t, T) = H(\mathcal{X}_{\hat{\rho}_A(t, T)}) + H(\mathcal{X}_{\hat{\rho}_B(t, T)}) - H(\mathcal{X}_{\hat{\rho}_{AB}(t, T)}), \quad (\text{A16})$$

where $H(\mathcal{X})$ denotes the Shannon entropy of the spectral (probability) distribution \mathcal{X} . Since we have $\mathcal{X}_{\hat{\rho}_A(t, T)} = \mathcal{X}_{\hat{\rho}_B(t, T)}$, the above equation can be simplified as

$$\mathcal{I}_{A:B}(t, T) = 2H(\mathcal{X}_{\hat{\rho}_A(t, T)}) - H(\mathcal{X}_{\hat{\rho}_{AB}(t, T)}). \quad (\text{A17})$$

-
- [1] S. Sachdev, *Quantum Phase Transitions* (Cambridge University Press, 2009).
- [2] B. K. Chakrabarti, A. Dutta, and P. Sen, *Quantum Ising phases and transitions in transverse Ising models* (Springer Berlin Heidelberg, 1996).
- [3] S. Suzuki, J. Inoue, and B. K. Chakrabarti, *Quantum Ising Phases and Transitions in Transverse Ising Models* (Springer Berlin Heidelberg, 2013).
- [4] K. Sengupta, S. Powell, and S. Sachdev, *Phys. Rev. A* **69**, 053616 (2004).
- [5] A. Sen(De), U. Sen, and M. Lewenstein, *Phys. Rev. A* **72**, 052319 (2005).
- [6] F. Pollmann, S. Mukerjee, A. G. Green, and J. E. Moore, *Phys. Rev. E* **81**, 020101 (2010).
- [7] M. Heyl, A. Polkovnikov, and S. Kehrein, *Phys. Rev. Lett.* **110**, 135704 (2013).
- [8] M. Heyl, *Phys. Rev. Lett.* **113**, 205701 (2014).
- [9] B. Žunkovič, M. Heyl, M. Knap, and A. Silva, *Phys. Rev. Lett.* **120**, 130601 (2018).
- [10] M. Heyl, *Phys. Rev. Lett.* **115**, 140602 (2015).
- [11] M. Heyl, *Rep. Prog. Phys.* **81**, 054001 (2018).
- [12] S. A. Weidinger, M. Heyl, A. Silva, and M. Knap, *Phys. Rev. B* **96**, 134313 (2017).
- [13] S. Vajna and B. Dóra, *Phys. Rev. B* **89**, 161105 (2014).
- [14] E. Canovi, E. Ercolessi, P. Naldesi, L. Taddia, and D. Vodola, *Phys. Rev. B* **89**, 104303 (2014).
- [15] S. Haldar, S. Roy, T. Chanda, A. Sen(De), and U. Sen, "Multipartite entanglement at dynamical quantum phase tran-

- sitions with non-uniformly spaced criticalities,” (2018), [arXiv:1811.12796](https://arxiv.org/abs/1811.12796).
- [16] L. Amico and D. Patanè, *Europhysics Letters (EPL)* **77**, 17001 (2007).
- [17] A. D. Rane, U. Mishra, A. Biswas, A. Sen(De), and U. Sen, *Phys. Rev. E* **90**, 022144 (2014).
- [18] A. W. Kinross, M. Fu, T. J. Munsie, H. A. Dabkowska, G. M. Luke, S. Sachdev, and T. Imai, *Phys. Rev. X* **4**, 031008 (2014).
- [19] E. Barouch, B. M. McCoy, and M. Dresden, *Phys. Rev. A* **2**, 1075 (1970).
- [20] S. Bhattacharyya, S. Dasgupta, and A. Das, *Scientific Reports* **5** (2015), 10.1038/srep16490.
- [21] R. Horodecki, P. Horodecki, M. Horodecki, and K. Horodecki, *Rev. Mod. Phys.* **81**, 865 (2009).
- [22] A. Osterloh, L. Amico, G. Falci, and R. Fazio, *Nature* **416**, 608 (2002).
- [23] T. J. Osborne and M. A. Nielsen, *Phys. Rev. A* **66**, 032110 (2002).
- [24] L. Amico, R. Fazio, A. Osterloh, and V. Vedral, *Rev. Mod. Phys.* **80**, 517 (2008).
- [25] M. Lewenstein, A. Sanpera, V. Ahufinger, B. Damski, A. Sen(De), and U. Sen, *Advances in Physics* **56**, 243 (2007).
- [26] M. Lewenstein, A. Sanpera, and V. Ahufinger, *Ultracold Atoms in Optical Lattices: Simulating quantum many-body systems* (Oxford University Press, 2017).
- [27] T. Chanda, T. Das, D. Sadhukhan, A. K. Pal, A. Sen(De), and U. Sen, *Phys. Rev. A* **94**, 042310 (2016).
- [28] S. Roy, T. Chanda, T. Das, D. Sadhukhan, A. Sen(De), and U. Sen, *Phys. Rev. B* **99**, 064422 (2019).
- [29] A. Peres, *Quantum Theory: Concepts and Methods (Fundamental Theories of Physics Book 57)* (Springer, 2006).
- [30] G. Vidal and R. F. Werner, *Phys. Rev. A* **65**, 032314 (2002).
- [31] M. B. Plenio, *Phys. Rev. Lett.* **95**, 090503 (2005).
- [32] A. Peres, *Phys. Rev. Lett.* **77**, 1413 (1996).
- [33] M. Horodecki, P. Horodecki, and R. Horodecki, *Phys. Lett. A* **223**, 1 (1996).
- [34] T. M. Cover and J. A. Thomas, *Elements of Information Theory (Wiley Series in Telecommunications and Signal Processing)* (Wiley-Interscience, New York, NY, USA, 2006) pp. 19–25.
- [35] L. Henderson and V. Vedral, *J Phys A: Mathematical and General* **34**, 6899 (2001).
- [36] B. Groisman, S. Popescu, and A. Winter, *Phys. Rev. A* **72**, 032317 (2005).
- [37] E. Lieb, T. Schultz, and D. Mattis, *Ann. Phys.* **16**, 407 (1961).
- [38] E. Barouch and B. M. McCoy, *Phys. Rev. A* **3**, 786 (1971).
- [39] E. Barouch and B. M. McCoy, *Phys. Rev. A* **3**, 2137 (1971).
- [40] T. Yu and J. H. Eberly, *Quantum Information & Computation* **7**, 459 (2007).
- [41] P. E. Mendona, M. A. Marchioli, and D. Galetti, *Annals of Physics* **351**, 79 (2014).